

The Origins of Noncovalent Catalysis of Intermolecular Diels–Alder Reactions by Cyclodextrins, Self-Assembling Capsules, Antibodies, and RNAses

Susanna P. Kim, Andrew G. Leach, and K. N. Houk*

Department of Chemistry and Biochemistry, University of California, Los Angeles, California 90095-1569

houk@chem.ucla.edu

Received December 26, 2001

The catalysis of Diels–Alder reactions by noncovalent binding by synthetic, protein, and nucleic acid hosts has been surveyed and compared. These catalysts consist of binding cavities that form complexes containing both the diene and the dienophile; the cycloaddition reaction occurs in the cavity. The binding requires no formation of covalent bonds and is driven principally by the hydrophobic (or solvophobic) effect. A molecular mechanics and dynamics study of the cyclodextrin catalysis of a Diels–Alder reaction is used to exemplify and probe this form of catalysis. Detailed kinetic data is available for catalysis by antibodies, RNA, cyclodextrins, and Rebek's tennis ball capsules. Some of these catalysts stabilize the reactants more than the transition state and consequently will only have catalytic effect under conditions of low substrate-to-catalyst ratios. None of the hosts achieve significant specific binding of transition states that is the hallmark of enzyme catalysis.

Introduction

The development of catalysts for useful organic reactions is one of the principle goals of contemporary chemical research. Acid–base catalysis, involving metal complexes, or metallic surfaces are among the most successful systems. Nevertheless, the use of stable and relatively unreactive organic substances as catalysts is a very attractive, if elusive, means to overcome the instabilities and toxicities associated with some of the successful catalysts.¹ Of particular interest is noncovalent catalysis—catalysis involving no covalent bonds between the catalyst and any of the reactants. Many enzymes effect reactions in precisely this way—by bringing together reactants in an active site without the formation of covalent bonds, and by presenting a host cavity highly complementary to the transition state.

A number of noncovalent catalysts for the Diels–Alder reaction have been reported. We have compared these and have discovered surprising similarities between seemingly disparate systems; acceleration arises predominantly from binding of reactants, converting a second-order reaction of diene with dienophile into a first-order reaction of the termolecular complex of host, diene, and dienophile, not from a special binding of transition states. This may be described as catalysis by an “entropy trap”, in the sense originally proposed by Westheimer (“by overcoming the unfavorable entropy of activation usually inherent in a chemical reaction”).² However, the definition of entropy traps was subsequently refined to mean systems providing concerted catalysis involving two functional groups in the same enzyme.³ Such a restricted

definition requires that the label of catalysis we study here be an example of “approximation.” Approximation has been defined as “the bringing together of two or more reactants in the active site.”³ The simultaneous presence of the two components of an intermolecular Diels–Alder reaction within the confined space of a cavity driven by host–guest interactions facilitates the reaction.

This paper first surveys the noncovalent Diels–Alder catalysts and then provides quantitative comparisons of the kinetics of catalysis. This mechanism of catalysis, in one representative case, has been probed with molecular mechanics calculations. Finally, noncovalent catalysis is compared with the familiar covalent catalysis provided by Lewis acids.

Background

We have recently found that the strength of binding of organic molecules by organic hosts in aqueous solution covers a surprisingly narrow range.⁴ The binding affinities of neutral organic guests with a large number of host types such as cyclodextrins, cyclophanes, crown ethers, and calixarenes in water are generally 10^4 M⁻¹ (90% fall within the range 10^1 – 10^6 M⁻¹). This corresponds to a ΔG of binding of -5 ± 4 kcal/mol. Even the binding of substrates by enzymes and catalytic antibodies ($\sim 1/K_m$) shows a median value of $\sim 10^4$ M⁻¹. Binding by macrocyclic hosts in nonaqueous solvents was found to be weaker and typically shows a K_a of $\sim 10^2$ M⁻¹. This behavior arises because the hydrophobic (or more generally, solvophobic) effect is limited by the amount of surface area that is buried away from the aqueous environment when a guest is bound into a host.

Enzymes and some catalytic antibodies manage to overcome these limitations and achieve potent binding

(1) (a) Ahrendt, K. A.; Borths, C. J.; MacMillan, D. W. C. *J. Am. Chem. Soc.* **2000**, *122*, 4243–4244 and references therein. (b) Paras, N. A.; MacMillan, D. W. C. *J. Am. Chem. Soc.* **2001**, *123*, 4370–4371. (c) Jen, W. S.; Wiener, J. J. M.; MacMillan, D. W. C. *J. Am. Chem. Soc.* **2000**, *122*, 9874–9875.

(2) Westheimer, F. H. *Adv. Enzymol.* **1962**, *24*, 441–482.

(3) Westheimer, F. H. *Adv. Phys. Org. Chem.* **1985**, *21*, 1–35.

(4) Houk, K. N.; Kim, S. P.; Leach, A. G.; Zhang, X.; Chen, J. Manuscript in preparation.

of transition states.⁵ This binding dwarves that of reactants and is frequently highly tuned to select one of many possible transition states. Organic chemists have endeavored to produce artificial catalysts that resemble enzymes.⁶ In this paper, we focus on those systems that catalyze a Diels–Alder reaction and make direct comparisons of all the noncovalent catalysts that have been studied kinetically.

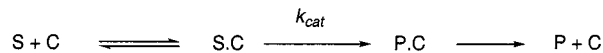
While enzyme-catalyzed Diels–Alder reactions have been proposed, there is still no conclusive evidence or kinetic data for such processes.⁷ Lovastatin nonaketide synthase, for instance, has recently been found to catalyze the intramolecular Diels–Alder reaction of a substrate analogue. Although a modest k_{cat} was measured (0.073 min^{-1}),^{7a} full kinetic characterization is still awaited.

We have identified four classes of “hosts” that accelerate the Diels–Alder reaction, for which detailed kinetic data are available—catalytic antibodies, RNA, cyclodextrins, and Rebek’s tennis balls. The Diels–Alder reaction has also been reported to be accelerated by micelles, albumin, and baker’s yeast,¹² but the lack of suitable kinetic data for these systems has prevented us from extending this study to these interesting systems.

The solubility of most of the catalyst types identified has necessitated these reactions to be performed in water. In fact, a pronounced acceleration of many Diels–Alder reactions has been observed in water itself relative to nonpolar solvents.¹³ This has been attributed to a combination of hydrophobic effects and selective hydrogen bonding to the transition state.^{14,15} Other solvents and Lewis acids promote the Diels–Alder reaction and vary its selectivity.^{9,16,17}

Kinetics of Catalysis of Diels–Alder Reactions by Noncovalent Binding. Michaelis–Menten kinetics are generally observed for enzymatic catalysis. The mecha-

Scheme 1. Michaelis–Menten Model for Enzymatic Catalysis by an Enzyme with Single Substrate^a



^a C is the catalyst (enzyme), S the substrate, and P the product of the reaction.

nism in Scheme 1 can be used to rationalize the kinetic profiles observed for enzymes processing a single substrate, S.¹⁸ Rapid precomplexation of substrate with catalyst, C, and dissociation of product, P, are assumed, with preferable binding of substrate over product. The substrate complex, S·C, reacts to form a product complex P·C with a rate constant k_{cat} .

This mechanism leads to the familiar equation

$$\left. \frac{d[P]}{dt} \right|_{t=0} = V_{\text{cat}} = \frac{k_{\text{cat}}[C]_0[S]}{K_M + [S]}$$

K_M is the substrate concentration necessary to achieve an initial rate that is half the maximum initial rate (V_{max} , the rate achieved at saturation of the catalyst). K_M can be interpreted as the dissociation constant for S·C.¹⁹ More accurately, it is the dissociation for all those substrate catalyst complexes that undergo reaction.

The corresponding (first order) rate (velocity, V) for the uncatalyzed reaction is

$$\frac{d[P]}{dt} = V_{\text{uncat}} = k_{\text{uncat}}[S]$$

The ratio of catalyzed to uncatalyzed rates is

$$\frac{V_{\text{cat}}}{V_{\text{uncat}}} = \frac{k_{\text{cat}}[C]_0[S]}{K_M + [S]} \cdot \frac{1}{k_{\text{uncat}}[S]} = \frac{k_{\text{cat}}[C]_0}{k_{\text{uncat}}\{K_M + [S]\}}$$

For acceleration to be observed, $V_{\text{cat}}/V_{\text{uncat}}$ must be greater than unity, and so $k_{\text{cat}}[C]_0 > k_{\text{uncat}}([S] + K_M)$. Alternatively, the condition $k_{\text{cat}}/k_{\text{uncat}} > ([S] + K_M)/[C]_0$ is necessary.

Catalysts with low $k_{\text{cat}}/k_{\text{uncat}}$ values make this condition of concentrations and substrate binding very difficult to achieve.

Cleland²⁰ and Dalziel²¹ have shown that for a two-substrate (S_1 and S_2) mechanism in which substrate binding and complex dissociation is more rapid than product formation from the termolecular substrate complex ($S_1 \cdot S_2 \cdot C$) and may occur in random order

$$V_{\text{cat}} = \frac{k_{\text{cat}}[S_1][S_2][C]_0}{K_{M1}K_{M2} + K_{M1}[S_2] + K_{M2}[S_1] + [S_1][S_2]}$$

where K_{M1} is the dissociation constant for S_1 to the empty catalyst cavity. For simplicity, we will assume that this is identical to K_{M1} for binding of S_1 to the catalyst containing S_2 . Scheme 2 shows this kinetic scenario schematically.

(18) Michaelis, L.; Menten, M. L. *Biochem. Z.* **1913**, 49, 333.

(19) Fersht, A. R. *Enzyme Structure and Mechanism*, 2nd ed.; W. H. Freeman: New York, 1984; pp 98–120.

(20) Cleland, W. W. *Enzymes* **1970**, 2, 1–65.

(21) Dalziel, K. *Enzymes* **1970**, 11, 2–60.

(5) (a) Radzicka, A.; Wolfenden, R. *Science* **1995**, 267, 90–93. (b) Raymond, J.-L. *Top. Curr. Chem.* **1999**, 200, 59–93.

(6) (a) Breslow, R. *Science* **1982**, 218, 532–537. (b) Breslow, R.; Dong, S. D. *Chem. Rev.* **1998**, 98, 1997–2011.

(7) (a) Auclair, K.; Sutherland, A.; Kennedy, J.; Witter, D. J.; Van der Heever, J. P.; Hutchinson, C. R.; Vederas, J. C. *J. Am. Chem. Soc.* **2000**, 122, 11519–11520. (b) Oikawa, H.; Kobayashi, T.; Katayama, K.; Suzuki, Y.; Ichihara, A. *J. Org. Chem.* **1998**, 63, 8748–8756. (c) Katayama, K.; Kobayashi, T.; Oikawa, H.; Honma, M.; Ichihara, A. *Biochim. Biophys. Acta* **1998**, 1384, 387–395. (d) Laschat, S. *Angew. Chem., Int. Ed. Engl.* **1996**, 35, 289–291.

(8) Hilvert, D.; Hill, K. W.; Nared, K. D.; Auditor, M.-T. M. *J. Am. Chem. Soc.* **1989**, 111, 9261–9262.

(9) Braisted, A. C.; Schultz, P. G. *J. Am. Chem. Soc.* **1990**, 112, 7430–7431.

(10) Yli-Kauhaluoma, J. T.; Ashley, J. A.; Lo, C.-H.; Tucker, L.; Wolfe, M. M.; Janda, K. D. *J. Am. Chem. Soc.* **1995**, 117, 7041–7047.

(11) Suckling, C. J.; Tedford, M. C.; Bence, L. M.; Irvine, J. I.; Stimson, W. H. *J. Chem. Soc., Perkin Trans. I* **1993**, 1925–1929.

(12) (a) Braun, R.; Schuster, F.; Sauer, J. *Tetrahedron Lett.* **1986**, 27, 1285–1288. (b) Rao, K. R.; Srinivasan, T. N.; Bhanumathi, N. *Tetrahedron Lett.* **1990**, 31, 5959–5960. (c) Colonna, S.; Manfredi, A.; Annunziata, R. *Tetrahedron Lett.* **1988**, 29, 3347–3350.

(13) (a) Rideout, D. C.; Breslow, R. *J. Am. Chem. Soc.* **1980**, 102, 7817–7818. (b) Grieco, P. A.; Garner, P.; He, Z. *Tetrahedron Lett.* **1983**, 24, 1897–1900. (c) Otto, S. *Catalysis of Diels–Alder Reactions In Water*. Doctoral thesis, Rijksuniversiteit Groningen, Groningen, The Netherlands, 1998, Chapter 1 (available from <http://www.chem.rug.nl/engberts>).

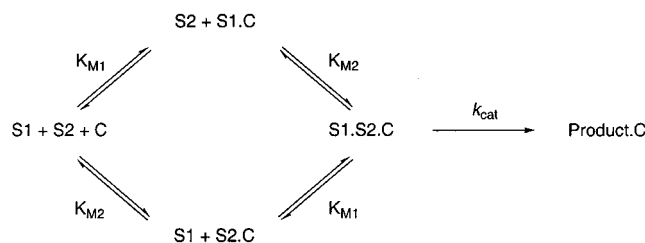
(14) Pindur, U.; Lutz, G.; Otto, C. *Chem. Rev.* **1993**, 93, 741–761.

(15) Kong, S.; Evansek, J. D. *J. Am. Chem. Soc.* **2000**, 122, 10418–10427 and references therein.

(16) (a) Otto, S.; Bertocin, F.; Engberts, J. B. F. N. *J. Am. Chem. Soc.* **1996**, 118, 7702–7707. (b) Otto, S. *Catalysis of Diels–Alder Reactions In Water*. Doctoral thesis, Rijksuniversiteit Groningen, Groningen, The Netherlands, 1998, Chapter 2 (available from <http://www.chem.rug.nl/engberts>).

(17) Kagan, H. B.; Riant, O. *Chem. Rev.* **1992**, 92, 1007–1019.

Scheme 2. Mechanism of the Reaction of Two Substrates, S1 and S2, Reacting through the Intermediacy of a Noncovalent Complex with Catalyst C^a



^a Each component has a complex with the catalyst with dissociation constant K_M .

In this case, the uncatalyzed reaction is second order and

$$V_{\text{uncat}} = k_{\text{uncat}}[S_1][S_2]$$

Therefore

$$\frac{V_{\text{cat}}}{V_{\text{uncat}}} = \frac{k_{\text{cat}}}{k_{\text{uncat}}} \cdot \frac{[C]_0}{K_{M1}K_{M2} + K_{M1}[S_2] + K_{M2}[S_1] + [S_1][S_2]}$$

Since K_{M1} and K_{M2} are often approximately 10^{-3} M for a large range of complexes⁴ and to be useful as a preparative method, $[S_1]$ and $[S_2]$ are both usually greater than 10^{-3} M, then

$$\frac{V_{\text{cat}}}{V_{\text{uncat}}} = \frac{k_{\text{cat}}}{k_{\text{uncat}}} \cdot \frac{[C]_0}{[S_1][S_2]}$$

If $k_{\text{cat}}/k_{\text{uncat}}$ is ≈ 1 , then $[C]_0$ must be greater than $[S_1][S_2]$ in order for catalysis to be observed. If for example, $[S_1] \approx [S_2] = 0.1$ M, then $[C]_0$ must be greater than 0.01 M. For a typical catalytic antibody, where $k_{\text{cat}}/k_{\text{uncat}} \approx 10^3$, then $10^3 [C]_0 = 10^{-2}$, or a catalyst concentration of greater than 10^{-5} will give $V_{\text{cat}} > V_{\text{uncat}}$.

In all circumstances, increasing $[C]$ enhances the catalyzed reaction in preference to the uncatalyzed reaction. Changing $[S_1]$ away from K_{M1} or $[S_2]$ away from K_{M2} can only be tolerated within the limits proscribed by $k_{\text{cat}}/k_{\text{uncat}}$ described above. The capability of each system to act as a catalyst is therefore determined by the value of $k_{\text{cat}}/k_{\text{uncat}}$; the higher this ratio, the broader the range of substrate concentrations that will involve more product generation through the catalyzed path than through the uncatalyzed path.

The value of $k_{\text{cat}}/k_{\text{uncat}}$ for a given catalyst and reaction system is a constant determined by the relative binding free energies of the substrate and transition state. k_{cat} corresponds to an activation free energy of ΔG_c^\ddagger and k_{uncat} corresponds to an activation free energy of ΔG_u^\ddagger . These are illustrated in Figure 1.

The value of $k_{\text{cat}}/k_{\text{uncat}}$ is maximized when $\Delta G_u^\ddagger - \Delta G_c^\ddagger$ is largest; the cycle in Figure 1 shows that this requires that $\Delta G_b(S) - \Delta G_b(\text{TS})$ is maximized. In principle, the substrate may even have a positive binding free energy, but if $k_{\text{cat}} = k_{\text{uncat}}$, then catalysis should only be observed when the concentration of catalyst exceeds that of substrate.

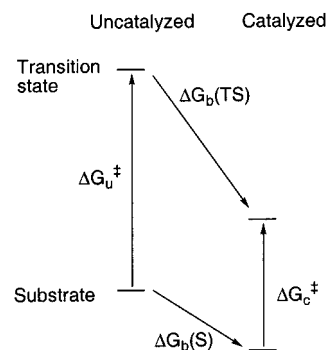
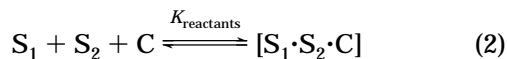


Figure 1. Free energy cycle for catalysis by binding of substrates and transition state.

We briefly survey the different catalytic host systems that we have identified for all-carbon Diels–Alder reactions. Each of the systems described has been the subject of detailed kinetic studies. We have processed the kinetic data in such a way that we can obtain Michaelis constants for both the diene and dienophile (K_{M1} and K_{M2}). These are either derived from kinetic measurements or from independent measurements of the dissociation constant for the complex of the catalytic host with either the diene or dienophile. We also present k_{uncat} , the second-order rate constant for the uncatalyzed Diels–Alder reaction, and k_{cat} , the first-order rate constant for the conversion of the termolecular host–diene–dienophile complex to form the host–product complex.

Table 1 summarizes these data for all of the systems. These data are illustrated graphically in Figure 2. This graph presents the data in a format analogous to that employed for enzymes by Wolfenden et al., all normalized relative to k_{uncat} .⁵ Deductions, discussed in detail below, can be made concerning the catalytic capabilities of the various systems by comparing the lengths of the bars in this logarithmic plot.

Preferential Binding of the Transition State over Reactants in Noncovalent Catalysis of Diels–Alder Reactions. The degree to which the transition state is stabilized with respect to the reactants can be extracted from the values of $k_{\text{cat}}/k_{\text{uncat}}$. This is equivalent to $K_{\text{TS}}/K_{\text{reactants}}$, where K_{TS} and $K_{\text{reactants}}$ are the equilibrium constants for reactions 1 and 2, respectively.^{5,22}



$\Delta G_{\text{binding}}(\text{TS}) - \Delta G_{\text{binding}}(\text{S}_1 + \text{S}_2)$ can be calculated from $k_{\text{cat}}/k_{\text{uncat}}$ (Figure 1) and is shown in Table 2. In some systems known to accelerate the Diels–Alder reaction, the actual degree to which this is attributable to specific stabilization of the transition state is limited. 1E9 and the cyclodextrin are the most effective systems by this measure. The acceleration achieved by a particular catalyst will depend on the relative values of K_M and the substrate and catalyst concentrations, as compared to the value of $k_{\text{cat}}/k_{\text{uncat}}$, as described above.

(22) (a) Mader, M. M.; Bartlett, P. A. *Chem. Rev.* **1997**, *97*, 1281–1301. (b) Fersht, A. R. *Enzyme Structure and Mechanism*, 2nd edition; W. H. Freeman: New York, 1984; pp 311–346.

Table 1. Kinetic Data and Binding Constants for the Noncovalent Catalysis of Intermolecular Diels–Alder Reactions

system	$K_M(\text{diene})$ [K_{M1}] (M)	$K_M(\text{dienophile})$ [K_{M2}] (M)	$K_{M1}K_{M2}$ (M^2)	k_{cat} (s^{-1})	k_{uncat} ($M^{-1}s^{-1}$)	$k_{\text{cat}}/k_{\text{uncat}}$ (M)	k_{cat}/K_{M1} ($M^{-1}s^{-1}$)	k_{cat}/K_{M2} ($M^{-1}s^{-1}$)	$k_{\text{cat}}/K_{M1}K_{M2}$ ($M^{-1}s^{-1}$)
1E9 ^a	2.4×10^{-3}	2.9×10^{-2}	7.0×10^{-5}	2.2×10^{-1}	2.2×10^{-4}	1000	9.0×10^1	7.5	3.1×10^3
39A11 ^b	1.1×10^{-3}	7.4×10^{-4}	8.4×10^{-7}	6.7×10^{-1}	1.9	0.35	5.9×10^2	9.1×10^2	8.0×10^5
13G5 ^c	2.7×10^{-3}	1.0×10^{-2}	2.7×10^{-5}	2.0×10^{-5}	2.9×10^{-6}	6.9	7.4×10^{-3}	2.0×10^{-3}	7.4×10^{-1}
4D5 ^c	1.6×10^{-3}	5.9×10^{-3}	9.4×10^{-6}	5.8×10^{-5}	1.2×10^{-5}	4.9	3.6×10^{-2}	9.8×10^{-3}	6.1
22C8 ^c	7.0×10^{-4}	7.5×10^{-3}	5.3×10^{-6}	5.3×10^{-5}	2.9×10^{-6}	18	7.6×10^{-2}	7.1×10^{-3}	1.0×10^1
7D4 ^c	9.6×10^{-4}	1.7×10^{-3}	1.6×10^{-6}	5.7×10^{-5}	1.2×10^{-5}	4.8	5.9×10^{-2}	3.4×10^{-2}	3.5×10^1
RNA(22a) ^d	^e	2.3×10^{-3}		1.1×10^{-2}	5.4×10^{-3}	2.0		4.8	
RNA(24) ^d	^e	2.9×10^{-5}		1.5×10^{-4}	5.4×10^{-3}	0.027		5.1	
RNA ^f	3.7×10^{-4}	8.0×10^{-3}	3.0×10^{-6}	3.5×10^{-1}	5.3×10^{-2}	6.6	9.5×10^2	4.4×10^1	1.2×10^5
CD ^g	3.1×10^{-3j}	3.1×10^{-3j}	9.8×10^{-6}	1.9^h	4.7×10^{-2}	40	6.1×10^2	6.1×10^2	1.9×10^5
CD ⁱ	6.3×10^{-3j}	6.3×10^{-3j}	4.0×10^{-5}	1.5×10^{1h}	1.5×10^{-1}	100	2.4×10^3	2.4×10^3	3.7×10^5
Tennis Ball ^k	2.1×10^{-1l}	2.3×10^{-3l}	4.9×10^{-4}	3.0×10^{-6}	6.3×10^{-6}	0.48	1.4×10^{-5}	1.3×10^{-3}	6.2×10^{-3}

^a Antibody 1E9 with substrates **1b** and **2** (15 °C). ^b Antibody 39A11 with substrates **5** and **6** (25 °C). ^c Antibody-catalyzed reactions at 37 °C. ^d Number in parentheses is the isolate number from set RNA catalysts prepared in ref 30 for reaction of RNA-linked diene with **10** (25 °C). ^e Not measurable as diene is bound to RNA catalyst. ^f RNA catalyst described in ref 31 for the acceleration of the reaction of **11** with **12** (25 °C). ^g β -Cyclodextrin catalyzing the reaction of cyclopentadiene with monoethyl fumarate (20 °C). ^h These are described as k_{cat} and as the rate of decomposition of the termolecular complex in ref 36, but the units given are appropriate for a zeroth order rate constant ($M s^{-1}$). It is assumed that these units are a typographical error. ⁱ β -Cyclodextrin catalyzing the reaction of cyclopentadiene with diethyl fumarate (20 °C). ^j It has been assumed that the apparent K_M described in the paper is an average for the diene and dienophile. ^k Rebek's tennis ball with cyclohexadiene and *p*-benzoquinone (22 °C). ^l This is $1/\sqrt{K}$ where K is the binding constant obtained for the 1:2 host/guest complex formed with two molecules of the diene or dienophile.

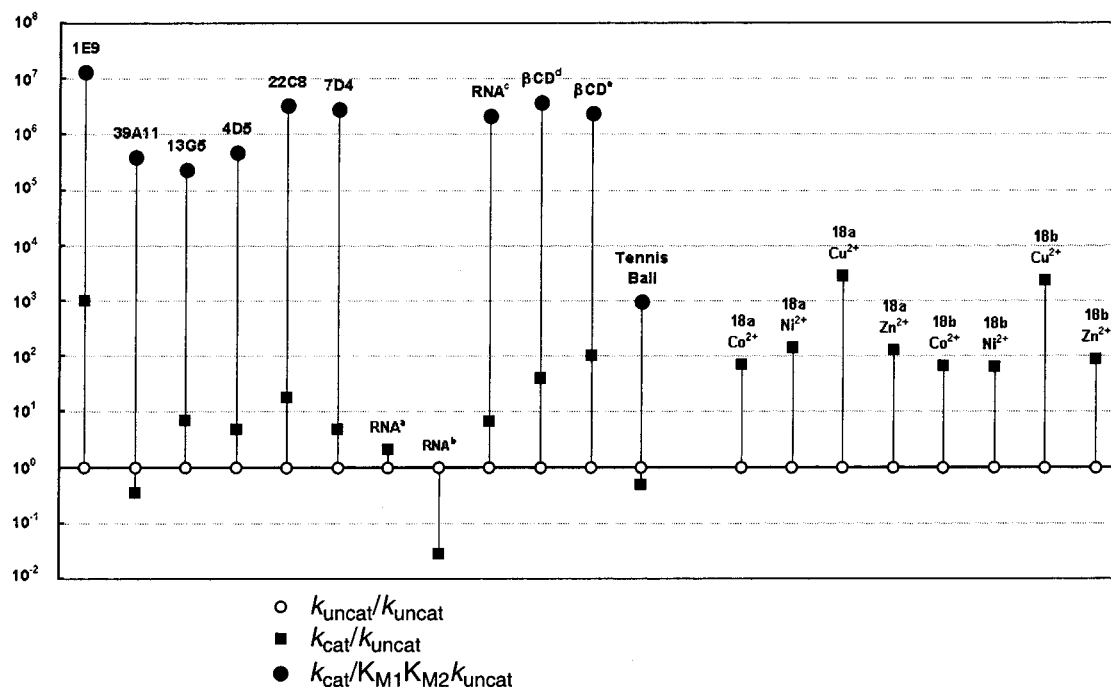


Figure 2. Graphical summary of the values of k_{cat} , k_{uncat} , and $k_{\text{cat}}/K_{M1}K_{M2}$ for the noncovalent catalyst systems and a comparison to the corresponding values of k_{cat} achieved by aqueous Lewis acid catalysts. All are normalized to be multiples of the appropriate k_{uncat} . The lines linking k_{uncat} (at the x -axis) to k_{cat} measure the acceleration that may be achieved under conditions of high substrate concentration (saturated catalyst). The lines linking k_{uncat} to $k_{\text{cat}}/K_{M1}K_{M2}$ indicate the acceleration that may be achieved under conditions of low substrate concentration.

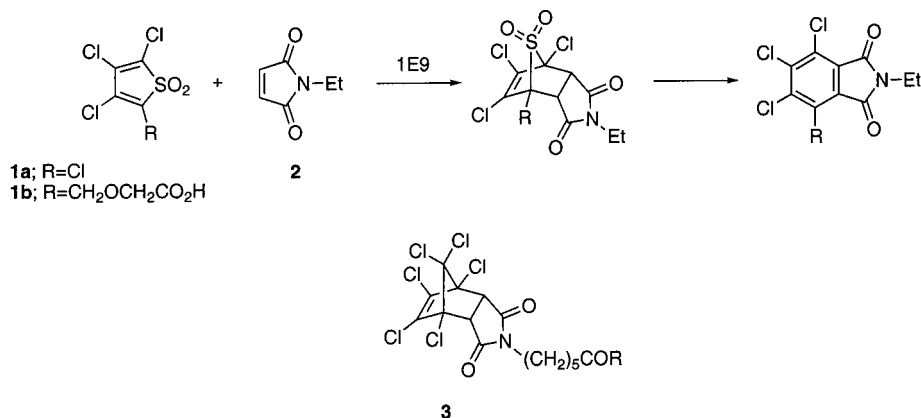
As can be seen from Table 2, 39A11, some of the RNA catalysts and the tennis ball actually stabilize the reactants more than they do the transition state. These are reflected in Figure 2, by the lower value of $k_{\text{cat}}/k_{\text{uncat}}$ than $k_{\text{uncat}}/k_{\text{uncat}}$. In terms of catalysis, the vertical line linking $k_{\text{cat}}/k_{\text{uncat}}$ to $k_{\text{uncat}}/k_{\text{uncat}}$ indicates the extent of catalysis under conditions of high substrate concentration ($[S_1] > K_{M1}$ and $[S_2] > K_{M2}$). Here there is acceleration, as long as $[C]_0 > [S_1][S_2]$.

The vertical distance to $k_{\text{cat}}/(K_{M1}K_{M2}k_{\text{uncat}})$ reflects the acceleration when substrate concentration is low. Here, there is acceleration so long as $[C]_0 > K_{M1}K_{M2}$. All of these, including those which do not show preferential binding

of the transition state, may be catalysts with low substrate and high catalyst concentration. It is clear from the $\Delta\Delta G$ values in Table 2 and the line lengths in Figure 1 that 1E9 is an outstandingly efficient system.²³ Despite this, the extra stabilization of the transition state is miniscule compared to the kind of preferential binding of transition states that may be expected for enzymes where values of 14 kcal/mol are typical.^{4,24}

(23) Chen, J.; Deng, Q.; Wang, R.; Houk, K. N.; Hilvert, D. *Chem-BioChem* **2000**, *1*, 255–261.

(24) Houk, K. N.; Leach, A. G.; Kim, S. P.; Chen, J. Manuscript in preparation.

Scheme 3. Diels–Alder Reaction Catalyzed by Antibody 1E9^a

^a The hapten **3** was used to elicit the antibody.

Table 2. Difference in Binding Free Energy between the Reactants and the transition state of a number of intermolecular Diels–Alder Reactions

	$\Delta G_{\text{binding}}(\text{TS}) - \Delta G_{\text{binding}}(\text{reactants})$ (kcal/mol)		$\Delta G_{\text{binding}}(\text{TS}) - \Delta G_{\text{binding}}(\text{reactants})$ (kcal/mol)
1E9	−4.0	RNA(22a) ^a	−0.4
39A11	+0.6	RNA(24) ^a	+2.2
13G5	−1.2	RNA ^b	−1.1
4D5	−1.0	CD(MEF) ^c	−2.2
22C8	−1.8	CD(DEF) ^d	−2.7
7D4	−1.0	tennis ball	+4.4

^a Reference 30. ^b Reference 31. ^c Reaction of monoethylfumarate with cyclopentadiene. ^d Reaction of diethylfumarate with cyclopentadiene.

Noncovalent Catalyst Types. (i) Catalytic Antibodies. Antibody 1E9 catalyzes the Diels–Alder reaction of thiophene dioxide, **1a**, and maleimide, **2** (Scheme 3). The antibody was elicited against hapten **3**, designed to mimic the Diels–Alder adduct.⁸ The product of the Diels–Alder reaction of **1a** and **2** extrudes SO₂ and then is rapidly oxidized in air and aromatizes. This removes any trace of regio- and stereoselectivity that may have been engendered by the antibody. Kinetic studies with a diene–dienophile pair chosen for their solubility (**1b** and **2**) facilitated the measurement of K_M , k_{cat} , and k_{uncat} in the standard way. Table 1 shows that the ratio of k_{cat} to k_{uncat} for 1E9 is larger than for any of the other systems reported in this paper. This remarkable catalytic capability has been explained by theoretical calculations, which show that 1E9 has a high degree of shape complementarity with the transition state.^{23,25} An asparagine residue in the active site can also form a hydrogen bond with one of the carbonyls of the dienophile; this hydrogen bond to the transition state is stronger than with the reactants. The binding of reactants by 1E9 is concluded to be driven by nonspecific hydrophobic effects, while the greater degree of stabilization of the transition state compared to reactants is attributed to electrostatic and shape complementarity between the active site and the transition state, evidenced by hydrogen bonds and other polar interactions. The involvement of these specific effects is the key reason that 1E9 is a more powerful catalyst than the others discussed in this paper. The other catalysts

do not exploit effectively polar interactions to selectively stabilize transition states.

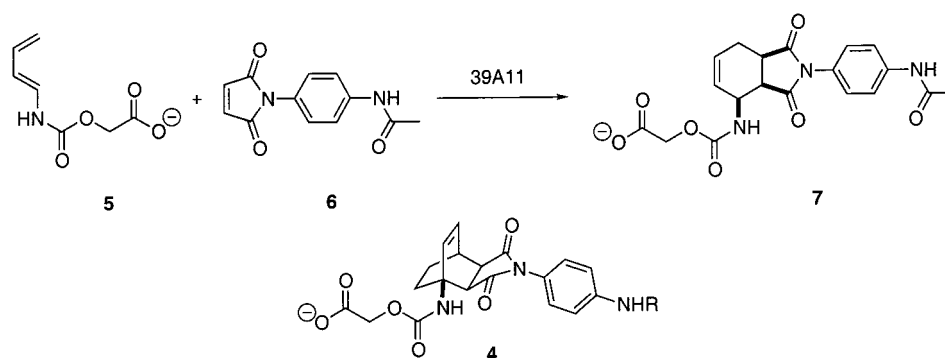
Antibody 39A11 catalyzes a different Diels–Alder reaction.⁹ It was designed to avoid product inhibition through use of a bicyclo[2.2.2]octene-based hapten, **4**, which resembles the boatlike transition state but is dissimilar to the chairlike product, **7**, of the reaction of **5** and **6** (Scheme 4).⁹ No details of the selectivity achieved by 39A11 were reported; kinetic measurements were made based on reaction carried to less than 3% completion. Antibody 39A11 achieves a reasonable binding of both the diene and dienophile (K_M is 1.1×10^{-3} M for the diene and 7.4×10^{-4} M for the dienophile) but has a poor k_{cat} to k_{uncat} ratio (0.35 M) and binds the reactants better than the transition state.

Antibodies 13G5 and 4D5 were elicited against the conformationally mobile ferrocene-based haptens **8a** and **8b**.¹⁰ When present in excess, 13G5 catalyzes the formation of the exo isomer of **9** with 95% ee (Scheme 5). Recent experiments show that when 13G5 is present in catalytic quantities (0.125 mol %) and the background reaction is accounted for, the antibody reaction proceeds with 98% ee, favoring the (3*S*,4*S*)-cyclohexene product.²⁶ Antibody 4D5, on the other hand, gave the endo isomer in a similar ee and, under catalytic conditions, catalyzed formation of the (3*S*,4*R*)-cyclohexene with an ee of 90%. Computational studies suggest that 13G5 achieves its stereoselective catalytic effect via hydrogen bonds between the carbamate NH and an aspartate residue and between the acrylamide carbonyl and a tyrosine OH.²⁶ An array of aromatic residues clamp the aromatic ring of the diene and prevent the endo transition states from fitting well into the active site. The enantioselectivity arises because the disfavored exo (*R,R*)-transition state is less complementary to the active site, especially with respect to the two aforementioned hydrogen bonds. Although these specific interactions play an important role in imparting selectivity, this involves primarily a fine tuning of the catalytic effect. As Table 2 shows, catalysis does not involve particularly significant selective binding of the transition state.

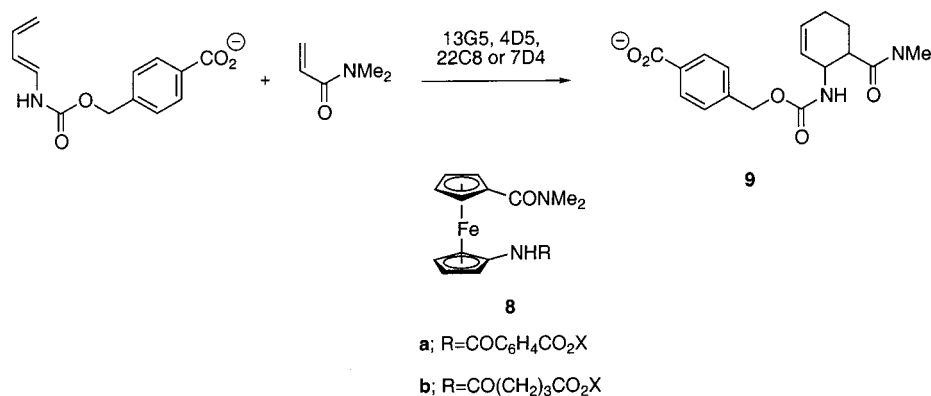
Catalytic antibodies for the same reaction (22C8 and 7D4) were elicited against bicyclo[2.2.2]octene-based haptens. Antibody 22C8 catalyzes formation of the exo isomer and 7D4 the endo isomer.¹⁰ The performance of

(25) Chen, J.; Wang, R.; Taussig, M.; Houk, K. N. *J. Org. Chem.* **2001**, *66*, 3021–3026.

(26) Cannizzaro, C. E.; Ashley, J. A.; Janda, K. D.; Houk, K. N. Manuscript in preparation.

Scheme 4. Diels–Alder Reaction Catalyzed by Antibody 39A11^a

^a Hapten **4** was used to elicit the antibody.

Scheme 5. Diels–Alder Reaction Catalyzed by Antibodies 13G5, 4D5, 22C8, and 7D4^a

^a Haptens **8a** and **8b** were used to elicit 13G5 and 4D5, respectively.

the four catalytic antibodies for this reaction are all very similar in terms of the values of K_M and k_{cat} that were obtained. All have moderate k_{cat}/k_{uncat} values, in the range 4–18 M.

The antibody H11 has also been shown to catalyze formation of Diels–Alder reaction products.¹¹ However, the mechanism by which this occurs has since been questioned,²⁷ and subsequent kinetic studies established that the process is intimately associated with an ester hydrolysis. Consequently, cycloaddition kinetics cannot be established.²⁸ A number of other catalytic antibodies for hetero-Diels–Alder reactions have also been established but these will not be discussed in detail.²⁹ Antibodies 9D9 and 10F11 catalyze the retro-Diels–Alder reaction of an anthracene–HNO adduct with K_M values of 165 and 256 μ M, respectively.^{29c,d} 10F11 has k_{cat}/k_{uncat} equal to 2505, for 9D9 k_{cat}/k_{uncat} is only 406. Antibody 309–1G7 catalyzes the Diels–Alder reaction of the two double bond isomers of 1,3-pentadiene with an aryl nitroso compound.^{29a,b} It achieves K_M values of 3–4 mM and k_{cat}/k_{uncat} ranges from 1200 for the trans isomer to 2600 for the cis isomer. k_{uncat} in these cases was measured under pseudo-first-order conditions.

(ii) Catalytic RNA (Ribozymes). Two successful catalytic RNA systems for the Diels–Alder reaction have so far been described.^{30,31} The NexStar group identified a number of RNA sequences that showed catalytic activity for the Diels–Alder reaction between a diene–tethered to the RNA via a poly(ethylene glycol) (PEG) spacer—and dienophile **10** (Scheme 6).³⁰ The intramolecular nature of the diene and catalyst prevented K_M being assessed in the usual way for the diene and limited kinetic measurements to those for one turnover. The reaction mixture included some metal ions, and Cu²⁺ was found to be important for activity. This was ascribed to Lewis acid behavior, although many other metal ions showed no activity.^{30c} For the series of catalytic RNAs, k_{cat} and K_M (dienophile) vary by a factor of 75 but the corresponding k_{cat}/K_M (dienophile) varies only from 77 to 364 M^{−1} min^{−1}. No comment concerning the regio- or stereoselectivity achieved by this catalytic system was made. k_{cat}/k_{uncat} varies from 0.027 to 2.0 M.

Another group established the sequence of an RNA catalyst for a Diels–Alder reaction.³¹ Initially, catalysis involved the reaction of an RNA-tethered diene, but the catalyst is also effective with **11** and **12** (Scheme 7). The ee of the product, **13**, was found to be 90%; when

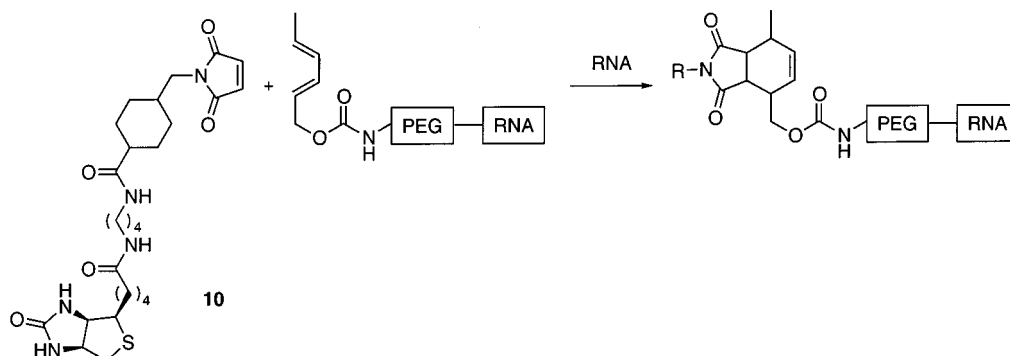
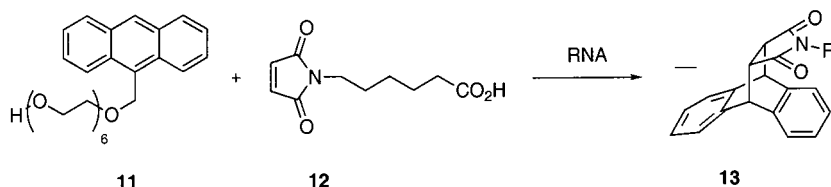
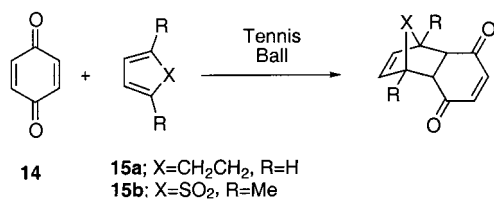
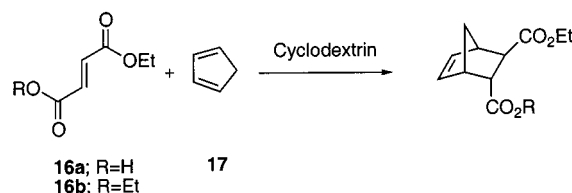
(27) Hilvert, D. *Acc. Chem. Res.* **1993**, 26, 552–558.

(28) (a) Khalaf, A. I.; Linaza, S.; Pitt, A. R.; Stimson, W. H.; Suckling, C. J. *Tetrahedron* **2000**, 56, 489–495. (b) Pitt, A. R.; Stimson, W. H.; Suckling, C. J.; Marrero-Tellado, J. J.; Vazzana, C. *Isr. J. Chem.* **1996**, 36, 171–175.

(29) (a) Meekel, A. A. P.; Resmini, M.; Pandit, U. K. *J. Chem. Soc., Chem. Commun.* **1995**, 571. (b) Resmini, M.; Meekel, A. A. P.; Pandit, U. K. *Pure and Appl. Chem.* **1996**, 68, 2025. (c) Bahr, N.; Güller, R.; Reymond, J.-L.; Lerner, R. A. *J. Am. Chem. Soc.* **1996**, 118, 3550. (d) Benschel, N.; Bahr, N.; Reymond, M. T.; Schenkels, C.; Reymond, J.-L. *Helv. Chim. Acta* **1999**, 82, 44–52.

(30) (a) Tarasow, T. M.; Tarasow, S. L.; Eaton, B. E. *Nature* **1997**, 389, 54–57. (b) Tarasow, T. M.; Tarasow, S. L.; Eaton, B. E. *J. Am. Chem. Soc.* **2000**, 122, 1015–1021. (c) Tarasow, T. M.; Tarasow, S. L.; Tu, C.; Kellogg, E.; Eaton, B. E. *J. Am. Chem. Soc.* **1999**, 121, 3614–3617.

(31) (a) Seelig, B.; Jäschke, A. *Chem. Biol.* **1999**, 6, 167–176. (b) Seelig, B.; Keiper, S.; Stuhlmann, F.; Jäschke, A. *Angew. Chem., Int. Ed.* **2000**, 39, 4576–4579. (c) Stuhlmann, F.; Jäschke, A. *J. Am. Chem. Soc.* **2002**, 124, 3238–3244.

Scheme 6. Diels–Alder Reaction Catalyzed by the NexStar RNA Based Catalyst (Ribozyme)**Scheme 7. Diels–Alder Reaction Catalyzed by an RNA-Based Catalyst****Scheme 8. Diels–Alder Reactions Catalyzed by Rebek's Tennis Ball****Scheme 9. Cyclodextrin-Catalyzed Diels–Alder Reaction**

corrected for the competing background reaction, the RNA was calculated to promote the reaction with 95% enantioselectivity. The enantiomeric RNA was also prepared, and it was found to provide the enantiomer of the Diels–Alder adduct. Product inhibition was significant. This RNA system binds the substrate very strongly; diene **11** has an association constant of $2.7 \times 10^3 \text{ M}^{-1}$ ($1/K_M = 1/3.7 \times 10^{-4}$). A $k_{\text{cat}}/k_{\text{uncat}}$ value of 6.6 M was achieved. A recently published investigation of this RNA catalyst concluded that association and catalysis are governed by hydrophobic effects for any substrate or transition state appropriately sized to fit into the active site.^{31c}

Tennis Ball Catalysis. Rebek has discovered shape-complementary molecules with appropriately placed functionality that form dimers held together by hydrogen bonding. He has styled one of these capsules the tennis ball.³² Recently, it was shown that these molecular containers can encapsulate diene and dienophile and accelerate the Diels–Alder reaction of *p*-benzoquinone **14** with cyclohexadiene or with 2,5-dimethylthiophene dioxide (**15**, Scheme 8).^{33,34} The reaction with cyclohexadiene suffers from product inhibition but, a full kinetic analysis was performed.³⁴ A low value of $k_{\text{cat}}/k_{\text{uncat}}$ (0.48 M) means that catalyst concentration must exceed substrate concentration. The tennis ball system is the only one described in this paper which involves a nonaqueous

solvent, *p*-xylene. Host–guest binding is generally weaker in organic solvents than in water,⁴ and the tennis ball system in xylene shows the weakest binding of all those reported in this paper: $K_M(\text{diene}) = 0.2 \text{ M}$.

Cyclodextrin Catalysis. Cyclodextrins catalyze a variety of organic reactions.^{6b,35} Catalysis of the reactions of dienophiles, **16**, with cyclopentadiene, **17**, follows Michaelis–Menten kinetics with saturation at high substrate concentration (Scheme 9).³⁶ Inhibition of the reaction was observed with hydrophobic dienophiles. A related study showed that significant changes in diastereoselectivity could be achieved by cyclodextrin catalysis along with tiny amounts of enantioselectivity.³⁸ The authors report one apparent K_M , which we have interpreted as an average for the diene and dienophile. The reported values of $3.1 \times 10^{-3} \text{ M}$ ($10^{-2.5} \text{ M}$) for **16a** and **17** and $6.3 \times 10^{-3} \text{ M}$ ($10^{-2.2} \text{ M}$) for **16b** and **17** are typical for any small molecule interacting with a cyclodextrin cavity. In general, cyclodextrin binding involves a K_D of $10^{-2.4 \pm 1.1} \text{ M}$.^{4,37} Cyclodextrin catalysis of a number of other Diels–Alder reactions has been reported, but the kinetics of these systems were not measured in sufficient detail to be included in this study.^{38,39}

(32) Wyler, R.; de Mendoza, J.; Rebek, J., Jr. *Angew. Chem., Int. Ed. Engl.* **1993**, 32, 1699–1701.

(33) Kang, J.; Santamaría, J.; Hilmersson, G.; Rebek, J., Jr. *J. Am. Chem. Soc.* **1998**, 120, 7389–7390.

(34) (a) Kang, J.; Hilmersson, G.; Santamaría, J.; Rebek, J., Jr. *J. Am. Chem. Soc.* **1998**, 120, 3650–3656. (b) Kang, J.; Rebek, J., Jr. *Nature* **1997**, 385, 50–52.

(35) Takahashi, K. *Chem. Rev.* **1998**, 98, 2013–2033.

(36) Schneider, H.-J.; Sangwan, N. K. *J. Chem. Soc., Chem. Commun.* **1986**, 1787–1789.

(37) Rekharsky, M. V.; Inoue, Y. *Chem. Rev.* **1998**, 98, 1875–1917.

(38) Schneider, H.-J.; Sangwan, N. K. *Angew. Chem., Int. Ed. Engl.* **1987**, 26, 896–897.

(39) (a) Rideout, D. C.; Breslow, R. *J. Am. Chem. Soc.* **1980**, 102, 7817–7818. (b) Breslow, R.; Guo, T. *J. Am. Chem. Soc.* **1988**, 110, 5613–5617.

Table 3. Enthalpies, Entropies, and Free Energies of Binding with β -Cyclodextrin for Reactants, Transition State, and Products for the Diels–Alder Reaction of 16b and 17 Estimated from Theoretical Studies

guest	gas phase			aqueous phase	
	$\Delta H_{\text{binding}}$	$\Delta S_{\text{binding}}$	$\Delta G_{\text{binding}}$	$\Delta \Delta G_{\text{solvation}}$	$\Delta G_{\text{binding}}$
cyclopentadiene	−3.8	−10	−0.8	−1.2	−2.1
diethyl fumarate	−25.5	−10	−22.5	+23.1	+0.6
cyclopentadiene + diethyl fumarate	−26.1	−20	−20.1	+19.0	−1.1
transition state	−25.4	−10	−22.4	+19.9	−2.5
product	−22.1	−10	−19.1	+23.3	+4.1

There have been computational studies of cyclodextrin complexation⁴⁰ and catalysis.⁴¹ The Diels–Alder reaction discussed above has received some theoretical attention.⁴¹ These calculations used a fixed host and guest structure and allowed them to interact via a Lennard-Jones potential function. Optimal complex structures and their corresponding energies were obtained, and it was predicted that cyclopentadiene binds more strongly than the less hydrophobic dienophiles. The calculated activation barriers (with AM1 transition states) were found to correlate well with experimental rate constants. The exception to this rule was diethyl maleate; this was attributed to the difference in shape of this Z-substituted olefin, which forces a different mode of binding to be employed.

Computational Study of Cyclodextrin Catalysis

To explore in detail the type of noncovalent catalysis discussed in this paper, we have performed a more detailed theoretical study of the cyclodextrin catalysis of the Diels–Alder reaction between cyclopentadiene and diethyl fumarate. Our aim was to identify the origins of noncovalent catalysis of the type discussed in this paper more quantitatively, for a relatively simple case, and to complement our earlier quantitative study of catalysis of a Diels–Alder reaction by antibody 1E9.²³ Force field optimizations and molecular dynamics, with MM2⁴² transition-state parameters for Diels–Alder reactions⁴³ and stochastic molecular dynamics, were all performed with the program suite MACROMODEL.⁴⁴

Molecules were placed inside the cyclodextrin cavity and optimized with the PRCG minimization routine. The optimum structure was then subjected to a molecular dynamics run (stochastic dynamics as implemented in MacroModel with step size 1.5 fs and total time 5 ns; the simulation temperature was set at 300 K, and the SHAKE algorithm was used to constrain all bond lengths). In this way, structures for the diene, dienophile, diene + dienophile, transition state, and product inside the cyclodextrin were obtained along with their corresponding energies averaged over a range of interaction orientations. The same species were then studied, using the same methods, outside the cyclodextrin. The energies calculated by these methods enabled us to compute enthalpies of complexation in the gas phase.

The key quantity is the free energy of complexation, and we have, therefore, estimated entropies of complexation. Bringing two molecules together in the gas phase (assumed to be their standard state) at standard temperature and concentration to form a loose complex in which the two molecules are free to move over the surface of one another eliminates one translational degree of freedom from each molecule. We estimate this to cost 10

eu.^{23,45} We assume that adding a further molecule, to make a termolecular complex, costs another 10 eu. By adding this gas-phase entropy of complexation as $-T\Delta S$ to ΔH , we obtain the gas-phase free energy of complexation (Table 3).

The binding energies are very large in gas-phase calculations. The GB/SA model for water was used to compute aqueous solvation free energies of each component and each cyclodextrin complex.⁴⁶ Binding free energies in water were obtained in this way. This methodology was verified by studying the known cyclodextrin complex of ethyl decanoate. The gas-phase calculations predict that for this ester, $\Delta H_{\text{binding}}$ is -11.3 kcal/mol. When the entropy is added and the GB/SA solvent model of water correction is included, $\Delta G_{\text{binding}}$ of -2.6 kcal/mol is predicted. The experimental aqueous phase value is -2.7 kcal/mol. All our calculations therefore employed this GB/SA model correction. The MM2 force field does not allow solvation effects to be calculated directly for the transition state, since the appropriate atomic radii necessary for this procedure have not been incorporated into the force field. These solvation corrections were estimated by performing the molecular dynamics calculations described above on a complex of cyclopentadiene and diethyl fumarate. This was constrained to maintain the C–C distances corresponding to the two forming bonds at the same values as in the transition state. The differences in free energy of solvation of the isolated complex and the complex inside the cyclodextrin was added as a solvation correction to the gas-phase free energy of complexation of the transition state. The energies of complexation for each system, calculated as described, are summarized in Table 3.

The absolute energies of the reactants, transition state and product using the MM2 force field cannot meaningfully be compared to one another; consequently, the same reaction was studied with B3LYP/6-31G*, which is known to reproduce energies of activation and energies of reaction for many pericyclic reactions.⁴⁷ The gas-phase free energy barrier for this reaction was predicted to be

(40) (a) Alvira, E.; Mayoral, J. A.; García, J. I. *Chem. Phys. Lett.* **1997**, *271*, 178–184. (b) Zubiari, M.; Jaime, C. *J. Org. Chem.* **2000**, *65*, 8139–8145. (c) Bonnet, P.; Jaime, C.; Morin-Allory, L. *J. Org. Chem.* **2001**, *66*, 689–692.

(41) (a) Alvira, E.; Cativiela, C.; García, J. I.; Mayoral, J. A. *Tetrahedron Lett.* **1995**, *36*, 2129–2132. (b) Luzhkov, V.; Åqvist, J. *Chem. Phys. Lett.* **1999**, *302*, 267.

(42) Allinger, N. L. *J. Am. Chem. Soc.* **1977**, *99*, 8127–8134 and subsequent additions.

(43) Spellmeyer, D. C.; Houk, K. N. *J. Org. Chem.* **1987**, *52*, 959–974.

(44) MacroModel V7.1 copyright Columbia University 1986–98, Schrödinger Inc., 1999: Mohamadi, F.; Richards, N. G. J.; Guida, W. C.; Liskamp, R.; Lipton, M.; Caufield, C.; Chang, G.; Hendrickson, T.; Still, W. C. *J. Comput. Chem.* **1990**, *11*, 440–467.

(45) Page, M. I.; Jencks, W. P. *Gazz. Chim. Ital.* **1987**, *117*, 455–460.

(46) Still, W. C.; Tempczyk, A.; Hawley, R. C.; Hendrickson, T. J. *Am. Chem. Soc.* **1990**, *112*, 6127–6129.

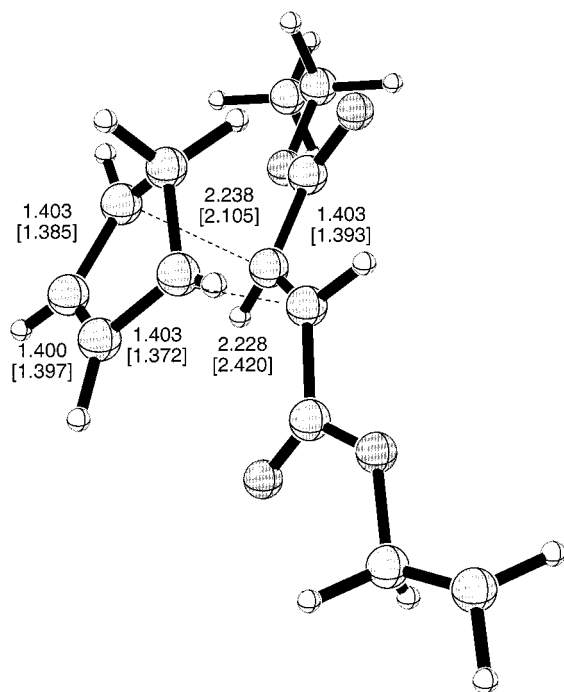


Figure 3. Transition structure for the Diels–Alder reaction between diethyl fumarate, **16b**, and cyclopentadiene, **17**. Distances (in Å) for the B3LYP/6-31G* transition structure are given along with those for the MM2* structure, which are reported in brackets.

27.0 kcal/mol.⁴⁸ A GB/SA solvation correction allowed prediction of the aqueous free energy barrier to be 28.1 kcal/mol. The energy of the bound transition state was obtained by adding the calculated free energy of complexation. B3LYP/6-31G* calculations also predicted that the reaction is exoergic by 1.9 kcal/mol. This was used to position the product and product complex at the correct energies relative to the reactants. The B3LYP transition state is shown in Figure 3. Geometrical comparisons with the MM2 structure show the two to be similar, although the MM2 transition state is rather more asynchronous than the B3LYP transition state. The total of the forming bond lengths for both structures indicate a similar degree of total bond formation. The calculations allow us to construct the free energy diagram for the reaction, shown in Figure 4.

Cyclopentadiene binds more favorably than diethyl fumarate in the cyclodextrin. Due to the GB/SA solvation correction for the aqueous environment, diethyl fumarate binding is predicted to be slightly unfavorable, with or

without cyclopentadiene in the cavity. The transition state for the cyclodextrin catalyzed reaction is bound better by nearly 3 kcal/mol, while the product of the reaction is unbound and will be released, making catalysis possible.

Our modeling predicts that $\Delta G_{\text{binding}}(\text{TS}) - \Delta G_{\text{binding}}(\text{reactants})$ is -1.4 kcal/mol, which is in reasonable agreement with the value of the experimentally obtained ratio of k_{cat} to k_{uncat} which corresponds to a $\Delta\Delta G$ of -2.7 kcal/mol (Table 2). The transition state of the reaction has a higher free energy of binding than the reactants, and this system will accelerate the reaction across a broad range of substrate concentrations. Furthermore, turnover can occur readily since the product is unbound.

The binding of nonpolar guests into a host is driven by hydrophobic (or solvophobic) effects. This is dependent on the surface area of hydrophobic molecules that can be buried out of contact with the solvent. This is shown dramatically by the increase in the binding energy of cyclopentadiene in cyclodextrin from gas phase (-0.8 kcal/mol) to aqueous solution (-2.1 kcal/mol) and the enormous decrease in diethyl fumarate binding, from -22.5 kcal/mol in the gas phase, to $+0.6$ kcal/mol in water. Our B3LYP calculations show that the dipole moment of the reactants (0.44 D for **17** and 0.07 D for **16b**) is less than that of the transition state (1.28 D), which in turn is less than that of the product (2.95 D). This mirrors the decrease in enthalpy of gas phase binding on going from reactants to transition state to products. During the dynamics simulation, the transition state and the diethyl fumarate form hydrogen bonds to the cyclodextrin quite frequently. This tendency is greatly reduced for the Diels–Alder adduct. The double bond of the fumarate is only slightly deflected from planarity ($\text{C}=\text{C}-\text{C}_{\text{ester}} \approx 130^\circ$) in the transition state and can therefore maintain many of the stabilizing interactions of the starting fumarate. However, the pyramidalization that takes place upon adduct formation ($\text{C}=\text{C}-\text{C}_{\text{ester}} \approx 115^\circ$) greatly alters the relative positioning in space of the two ester groupings. The adduct is therefore less well able to exploit the very good fit of the reactant complexes or the transition state and is less well able to form hydrogen bonds to the cyclodextrin cavity.

Our calculations are rough estimates; notably, our assumption of a constant gas-phase entropy of complexation masks significant variations. Nevertheless, we can draw some qualitative conclusions about this type of binding and noncovalent catalysis. Entropy favors the CD/TS complex more than the CD/reactants complex, because the CD/TS complex is bimolecular and the CD/reactant is termolecular. A host that can bind the two reactants of a bimolecular reaction can offer such an “entropy trap” to accelerate the reaction.

Discussion

All of the kinetic data obtained for the various systems discussed above have been abstracted and summarized in Table 1. The data are presented in a more convenient form in Figure 2, which allows a rapid visual assessment of the relative merits of each catalyst system to be made. The values of k_{cat} and $k_{\text{cat}}/K_{\text{M1}}K_{\text{M2}}$ are plotted as multiples of k_{uncat} on a logarithmic scale. The length of the line joining k_{uncat} (at the x axis) to k_{cat} gives a measure of the rate enhancement that will be provided per catalyst

(47) (a) Wiest, O.; Montiel, D. C.; Houk, K. N. *J. Phys. Chem. A* **1997**, *101*, 8378–8388. (b) Houk, K. N.; Beno, B. R.; Nendel, M.; Black, K.; Yoo, H. Y.; Wilsey, S.; Lee, J. K. *THEOCHEM* **1997**, *398–399*, 169–179.

(48) Structures were optimized and characterized by a frequency calculation. Gaussian 98 (Revision A.7): Frisch, M. J.; Trucks, G. W.; Schlegel, H. B.; Scuseria, G. E.; Robb, M. A.; Cheeseman, J. R.; Zakrzewski, V. G.; Montgomery, J. A., Jr.; Stratmann, R. E.; Burant, J. C.; Dapprich, S.; Millam, J. M.; Daniels, A. D.; Kudin, K. N.; Strain, M. C.; Farkas, O.; Tomasi, J.; Barone, V.; Cossi, M.; Cammi, R.; Mennucci, B.; Pomelli, C.; Adamo, C.; Clifford, S.; Ochterski, J.; Petersson, G. A.; Ayala, P. Y.; Cui, Q.; Morokuma, K.; Malick, D. K.; Rabuck, A. D.; Raghavachari, K.; Foresman, J. B.; Cioslowski, J.; Ortiz, J. V.; Stefanov, B. B.; Liu, G.; Liashenko, A.; Piskorz, P.; Komaromi, I.; Gomperts, R.; Martin, R. L.; Fox, D. J.; Keith, T.; Al-Laham, M. A.; Peng, C. Y.; Nanayakkara, A.; Gonzalez, C.; Challacombe, M.; Gill, P. M. W.; Johnson, B. G.; Chen, W.; Wong, M. W.; Andres, J. L.; Head-Gordon, M.; Replogle, E. S.; Pople, J. A. Gaussian, Inc., Pittsburgh, PA, 1998.

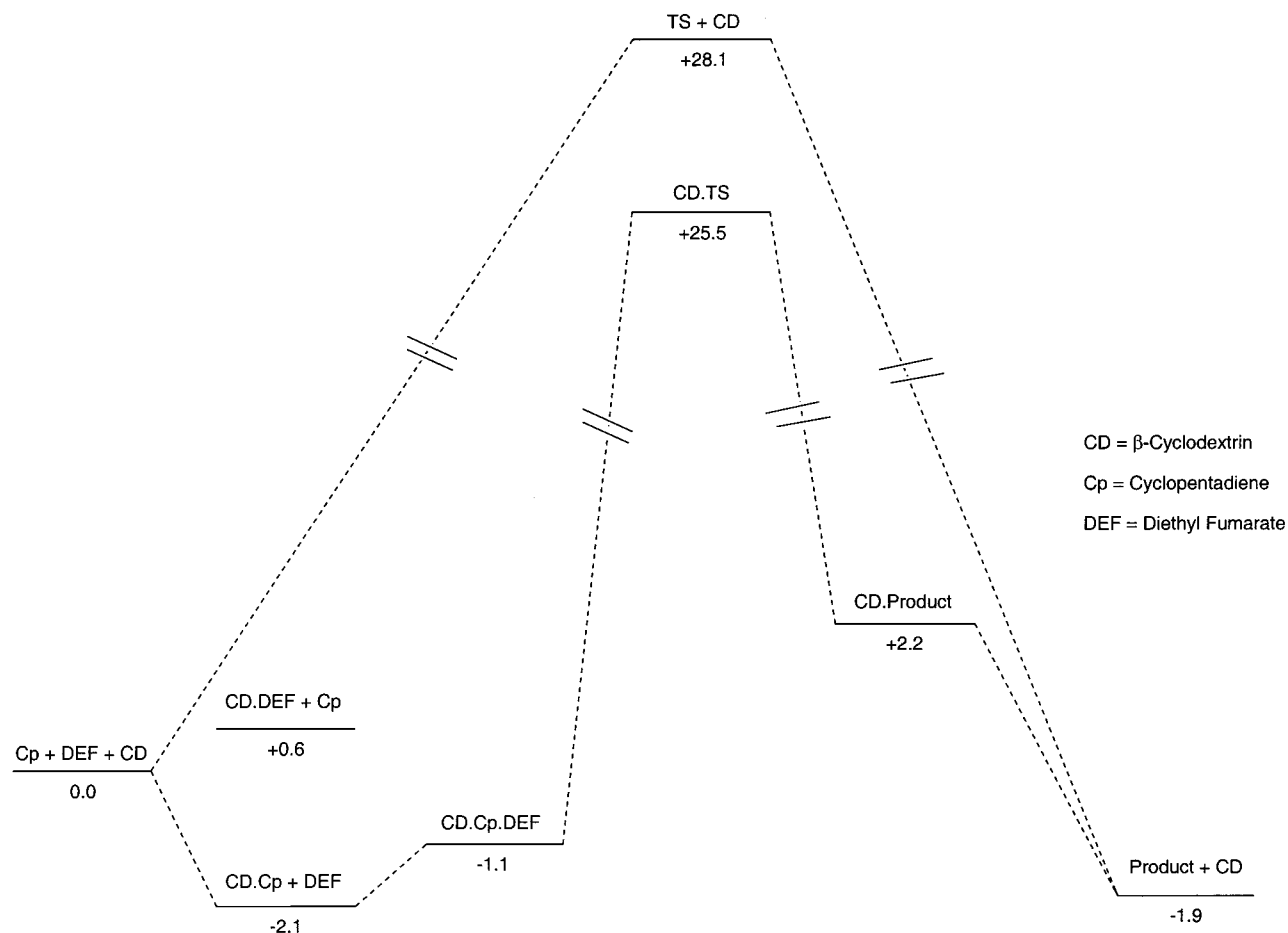


Figure 4. Reaction free energy diagram for the uncatalyzed (top line) and cyclodextrin-catalyzed (lower line) Diels–Alder reaction between diethyl fumarate, **16b**, and cyclopentadiene, **17**. Free energies are calculated using the MM2* force field combined with B3LYP/6-31G* and are given in kcal/mol and the GB/SA solvent model for water is used throughout. Standard temperature, pressure, and standard state are assumed throughout. Diagram not to scale.

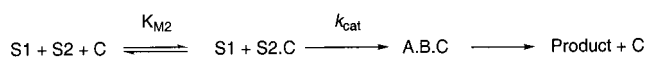
molecule when the substrate concentrations are high (relative to the appropriate K_M).

This value of $k_{\text{cat}}/k_{\text{uncat}}$ (which has units M) is equal to the maximum value of $[S_1][S_2]/[C]$ that can be tolerated before the uncatalyzed reaction begins to dominate. The longer this line, the lower the concentration of catalyst required. Thus, 39A11, one of the RNAs and the tennis ball will be ineffective at high substrate concentration unless this is matched by a higher catalyst concentration.

The line joining k_{uncat} to $k_{\text{cat}}/K_{M1}K_{M2}$ measures the acceleration that can be achieved per catalyst molecule when $[S_1] < K_{M1}$ and $[S_2] < K_{M2}$. The length of the line is equal to $1/[C]$, the inverse of the catalyst concentration that marks the border between enhancing the catalyzed and uncatalyzed reactions. The longer the line, the lower the catalyst concentration required for the catalyzed reaction to dominate. It is clear that all of the catalysts may be more easily effective in these conditions of low substrate concentration, even if they would be ineffective otherwise. It can also be seen at a glance that two of the RNA catalysts and the tennis ball are considerably less effective catalysts than the remaining systems. Of the other catalysts, most would accelerate reactions to a comparable extent under normalized conditions. 1E9 is the most effective of the noncovalent catalyst systems that we have studied.

Comparisons to Lewis Acid Catalysis. The Lewis acid catalysis of Diels–Alder reactions is well-known.

Scheme 10. Generic Reaction Scheme for Reactions Proceeding through One or More Precomplexation Events



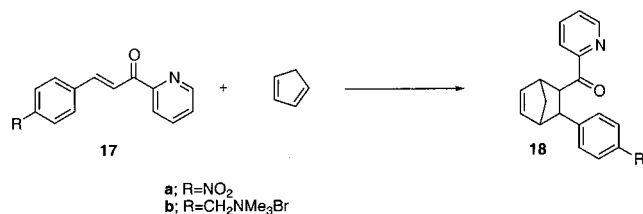
Generally, this involves aluminum halides or titanium halides coordinating to carbonyl groups of a dienophile in relatively nonpolar solvents. We have discussed mainly aqueous solvation, and Lewis-acid catalysis here is relatively rare. However, catalysis of some Diels–Alder reactions by soluble salts containing Lewis acidic metal ions have been reported, and that is compared here to noncovalent catalysis.

Lewis acid catalysis can be described by Scheme 10, which shares some features with that for noncovalent catalysts described above. S_1 and S_2 represent the diene and dienophile, respectively, and S_2 is assumed to bind more strongly. C represents the catalyst.

The rate equation, assuming the steady-state approximation for $S_2 \cdot C$ and rapid preequilibration, reduces to

$$V_{\text{Lewis acid}} = \frac{k_{\text{cat}}[S_1][S_2][C]}{K_{M2}}$$

Engberts has described the Diels–Alder reaction of a number of bidentate dienophiles, **17**, with cyclopentadi-

Scheme 11. Aqueous Lewis Acid Catalyzed Diels–Alder Reactions Reported by Engberts et al.**Table 4. [$k_{\text{cat}}/K_{\text{M2}}$]/ k_{uncat} (M) for Aqueous Lewis Acid Catalysis of Diels–Alder Reactions with Cyclopentadiene**

dienophile	Co ²⁺	Ni ²⁺	Cu ²⁺	Zn ²⁺
17a	6.1×10^3	4.5×10^4	1.2×10^6	4.3×10^3
17b	5.2×10^3	3.2×10^4	2.1×10^6	4.5×10^3

Table 5. Values of $k_{\text{cat}}/k_{\text{uncat}}K_{\text{M1}}K_{\text{M2}}$ for the Noncovalent Catalysis Systems

	$\frac{k_{\text{cat}}}{K_{\text{M1}}K_{\text{M2}}} \cdot \frac{1}{k_{\text{uncat}}}$
1E9	1.4×10^7
39A11	4.2×10^5
13G5	2.5×10^5
4D5	5.2×10^5
22C8	3.5×10^6
7D4	2.9×10^6
RNA	2.2×10^6
CD(MEF) ^b	4.1×10^6
CD(DEF) ^c	2.5×10^6
Tennis Ball	9.9×10^2

^a Reference 31. ^b Reaction of monoethylfumarate with cyclopentadiene. ^c Reaction of diethylfumarate with cyclopentadiene.

ene in water.¹⁶ This was compared to the reaction in organic solvents. The studies were extended to catalysis by Lewis acidic metal salts in water—Cu²⁺, Co²⁺, Zn²⁺, and Ni²⁺ (Scheme 11) are the Lewis acids, in their hydrated form. This was described in terms of a mechanism similar to that in Scheme 10 and a second-order rate constant, corresponding to k_{cat} , and the K_{M2} were measured. Unfortunately, the instability of the dienophiles limited the number of cases for which the background reaction could be studied to obtain k_{uncat} . The values of $k_{\text{cat}}/K_{\text{M2}}$ are compared to the available k_{uncat} data in Table 4, and values of $k_{\text{cat}}/k_{\text{uncat}}$ are plotted in Figure 2 alongside those for the noncovalent catalysts, taken from Table 5.

In the case of the rapidly equilibrating binding systems that effect noncovalent catalysis, it was shown earlier that for acceleration to be achieved, that $k_{\text{cat}}/k_{\text{uncat}}$ is best maximized as this makes the substrate binding and substrate and catalyst concentration requirements less stringent. In the case of Lewis acid catalysis, in order that the rate of product formation via the catalyzed reaction be higher than via the uncatalyzed reaction

$$\frac{k_{\text{cat}}}{k_{\text{uncat}}} > \frac{K_{\text{M2}}}{[\text{C}]}$$

or

$$\frac{k_{\text{cat}}}{k_{\text{uncat}}K_{\text{M2}}} > \frac{1}{[\text{C}]}$$

The values in Tables 4 and 5 of $k_{\text{cat}}/k_{\text{uncat}}K_{\text{M2}}$ for the Lewis acids and $k_{\text{cat}}/(k_{\text{uncat}}K_{\text{M1}}K_{\text{M2}})$ for the noncovalent

catalysts indicate $1/[\text{C}]$, the inverse of the minimum catalyst concentration which must be employed for catalysis to prevail. It is clear from these values that Lewis acid catalysis in water is at best unremarkably better than the noncovalent catalytic methods described above. This conclusion may seem surprising but it should be borne in mind that the aqueous environment precludes the use of the best Lewis acids for which K_{M2} will be much lower. The aqueous environment itself also greatly facilitates the Diels–Alder reaction such that k_{uncat} is larger than it would otherwise be.¹³ The k_{uncat} value for the reaction of 17a in acetonitrile is almost 300 times less than in water. Also notable is that the Cu²⁺-dependent RNA catalyst described earlier achieves catalysis much less dramatically than purely Lewis acidic catalysis by Cu²⁺.³⁰ Engberts' studies have been extended to catalysis by Lewis acids combined with micelles and vesicles and show that the effect of preconcentrating reactants combined with Lewis acid catalysis can be very dramatic.⁴⁹

Conclusions

Noncovalent catalysis of the Diels–Alder reaction has been achieved by a number of catalytic antibodies, ribozymes (RNA), cyclodextrins and Rebek's tennis ball. Each has been shown to follow Michaelis–Menten kinetics for which values of k_{cat} , K_{M1} for the diene, and K_{M2} for the dienophile have been measured. The binding of substrates in each of these cases is unexceptional, as all K_{M} values fall in the $\sim 10^{-3}$ M range expected for normal organic host–guest complexation in water.

Enzymes also bind substrates with the same magnitude of binding constants. However, they achieve substantially greater binding of transition states. In contrast, we find that the noncovalent catalyst systems we have studied bind transition states to approximately the same degree as substrates. Some are found to bind their transition states more weakly than the substrates. Enhanced rates of these bimolecular reactions may still be observed if the substrate concentration is reduced and the catalyst concentration increased.

Molecular modeling of one of the most efficient catalytic systems so far reported, employing a cyclodextrin cavity, has been used to exemplify the general phenomenon of noncovalent catalysis. The pre-binding of substrates provides an entropic advantage; the entropy that must usually be paid to bring substrates to a reactive transition state in solution has already been paid in large part during the binding process. The entropic penalty of binding is offset by the solvophobic effect.

Acknowledgment. We thank the UK Fulbright Commission and AstraZeneca (for a fellowship to A.G.L.) and the National Institute of General Medical Sciences, National Institutes of Health, for financial support of this research.

JO011180D

(49) (a) Otto, S.; Engberts, J. B. F. N.; Kwak, J. C. T. *J. Am. Chem. Soc.* **1998**, *120*, 9517–9525. (b) Rispens, T.; Engberts, J. B. F. N. *Org. Lett.* **2001**, *3*, 941–943. (c) Otto, S. *Catalysis of Diels–Alder Reactions In Water*. Doctoral thesis, Rijksuniversiteit Groningen, Groningen, Netherlands, 1998; Chapter 5 (available from <http://www.chem.rug.nl/engberts>).